

## Nanostructured Pt-Ru / Ionic Liquid Crystal Composite for Electrocatalytic Oxidation of Methanol

Mohammad H. BinSabt<sup>1</sup>, Nada F. Atta<sup>2\*</sup>, Yousef M. Ahmed<sup>2</sup>, Ahmed Galal<sup>2</sup>

<sup>1</sup> Chemistry Department, Faculty of Science, Kuwait University, 13060-Safat, Kuwait

<sup>2</sup> Chemistry Department, Faculty of Science, Cairo University, Giza 12613, Egypt

\*E-mail: [anada@sci.cu.edu.eg](mailto:anada@sci.cu.edu.eg)

Received: 8 August 2017 / Accepted: 22 September 2017 / Published: 12 November 2017

---

In this work, we report a highly active and durable methanol oxidation electrocatalyst, for the first time, based on the synergy of platinum-ruthenium-ionic liquid crystal (Pt-Ru-ILC). The incorporation of ionic liquid crystal played a main role resulting in quite uniform and ordered surface arrays. The ILC allowed more available catalytic sites while providing high ionic conductance surface. The efficiency of methanol oxidation increases while realizing the removal of carbonaceous poisoning products from the catalyst surface. The crystalline nature of piperidinium ILC resulted in the nucleation of nano-catalyst with an average size of 3 nm. Compared to other nano-catalysts, Pt-Ru-ILC displayed an  $I_F/I_R$  ratio of 12.2 with relatively higher current densities and lower methanol oxidation potential. A promising long-term durability and stability were also realized by the present catalyst.

---

**Keywords:** Methanol fuel cell; Ionic liquid crystals; Pt-Ru nanoparticles; Carbonaceous poison; Electrocatalyst.

### 1. INTRODUCTION

Electrooxidation of methanol has been a focus of current researchers due to several advantages, such as high efficiency, low polluting emissions, a potentially renewable fuel source, and convenient refueling [1–4]. The development of direct methanol fuel cells (DMFCs) is useful for power sources for transportation, portable electronics and other applications. One of the impeding problems in the commercialization is perhaps the high over-potential associated with the direct electro-oxidation of methanol at most unmodified surfaces [5]. The electrode material is obviously an important factor where a highly efficient electrocatalyst is needed.

Platinum (Pt) have been demonstrated as high performance catalysts for various fuel cells due to their anisotropic structure and unique surface properties [6–9]. The incorporation of a second metal

is needed to provide oxygen containing compounds when applying less potential values and results in weaker bond strength of Pt-CO which is a necessary step for the oxidative removal of adsorbed CO from the surface of platinum and helps the oxidation removal of CO to CO<sub>2</sub> [10]. The most studied bimetallic Pt-Ru catalysts with a low Ru content have been demonstrated to be much more effective in the electro-oxidation of methanol [11–13]. Among the preparation methods for Pt-Ru alloys, electrodeposition method has received great interest because of better control and ease of processing. The catalysts made by one-step electrodeposition method, exhibit high electro-catalytic performance towards methanol oxidation. These methods are effective in terms of the resulting materials with excellent purity and uniform size [13–16].

Recently, the use of ionic liquid (IL) thin films as reactivity-modifying coatings has received much attention, both in heterogeneous catalysis [17–22] and in electrocatalysis [23–25]. The properties of ionic liquid crystals can differ significantly from those of conventional, neutral ionic liquids. In addition, ionic liquid crystals (ILCs) are combining both the technological properties of ionic liquids and liquid crystals. ILCs are anisotropic materials that consist of solely ions (cations and anions). It has been shown that a mesophase can be induced and also the incorporation of charged units can enhance its stability [26–28]. One of the most promising features of ionic liquid crystals is ionic conductivity. To the best of our knowledge no papers mentioned the use of ionic liquid crystal for electro-oxidation of methanol or other fuels.

In the present work, we introduce for the first time a modified glassy electrode based on ionic liquid crystal/Pt-Ru nanostructures for the electrocatalytic oxidation of methanol in alkaline medium. In this study we indicate the role and the synergism of the ionic liquid crystal and the nanoparticles for electro-oxidation of methanol.

Each component of the composite fulfills an important role: Pt to serve as the active sites for methanol oxidation; Ru to facilitate the oxidative removal of carbonaceous poisons on adjacent metal sites; and the ILC to provide high electric conductivity and reasonable ordered surface needed for fast electrocatalysis. We believe that the present study introduces a novel and insightful approach to develop an effective and durable composite for direct methanol fuel cells.

## **2. EXPERIMENTAL**

### *2.1. Materials and reagents*

All chemicals were used as received without further purification. Perchloric acid, sulfuric acid, nitric acid, hydrochloric acid, methanol, hexachloroplatinic acid, 1-Butyl-1methylpiperidinium hexafluorophosphate ionic liquid crystal (ILC), 1-n-Hexyl-3-methylimidazolium tetrafluoroborate(IL), Palladium (II) chloride and ruthenium (III) chloride, Potassium hydroxide (KOH) , were purchased from Sigma-Aldrich (USA). All solutions were prepared from analytical grade chemicals and deionized water.

## 2.2. Electrochemical cell and equipment

Electrochemical characterization was carried out with a standard three-electrode/one compartment glass cell. The working electrode was a GC electrode ( $\phi$ : 3 mm) from (BASi, USA), a 6.0 cm long ( $\phi$  = 0.5 mm) Pt wire from Alfa Aesar (USA) was used as the auxiliary electrode and all the potentials in the electrochemical studies were referenced to Ag/AgCl (4 M KCl saturated with AgCl) electrode from (BASi, USA). All experiments were performed at  $25 \text{ }^\circ\text{C} \pm 0.2 \text{ }^\circ\text{C}$ . The GC electrode was polished with a (2  $\mu\text{m}$ )-alumina–water slurry until no visual scratches were observed. The electrochemical characterization was performed using a BAS epsilon-electrochemical analyzer (BASi, USA) (with  $\pm 5$  mV error).

The microstructure of the samples was investigated using Quanta FEG 250 (USA) instrument and an EDAX coupled to SEM was used to analyze the composition of the prepared samples (samples were prepared on GC sheet). High resolution transmission electron microscope (HR-TEM, Tecnai G20, FEI, Netherland) operated at 200 kV with LaB6 gun was utilized to characterize the size and microstructure of the prepared samples. Atomic force microscope (AFM) was measured using a Shimadzu Wet-SPM (Japan) scanning probe microscope.

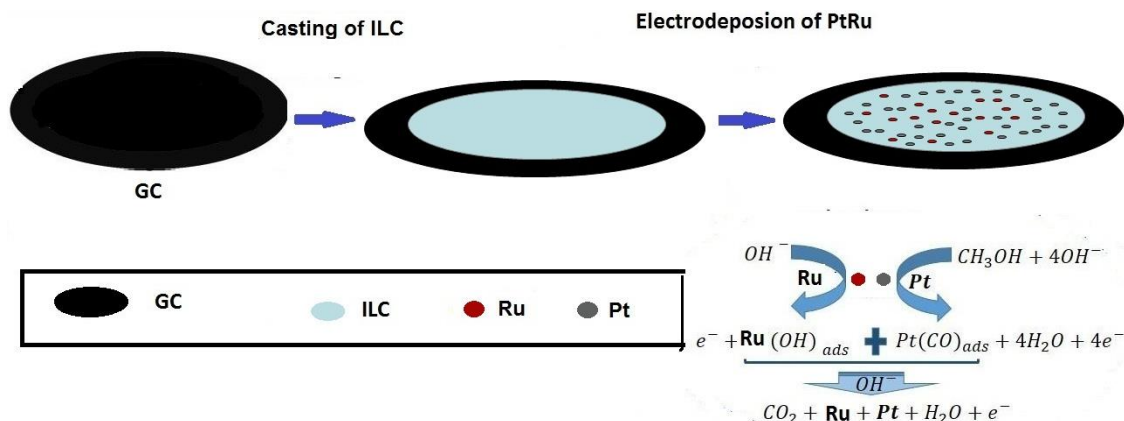
## 2.3 Preparation of catalysts solution

Platinum–palladium (Pt-Pd) co-catalysts was prepared by dissolving  $\text{H}_2\text{PtCl}_6$  and  $\text{PdCl}_2$  (with a ratio equivalent to (3)Pt:(1)Pd in aqua regia. The formed solution was heated until one-fourth of the original volume was reached by evaporation. The remaining solution was diluted to the required volume and concentration by 0.1 M perchloric acid. While, platinum or platinum-ruthenium (Pt-Ru) was prepared by dissolving  $\text{H}_2\text{PtCl}_6$  or a mixture of  $\text{H}_2\text{PtCl}_6$  and  $\text{RuCl}_3$  in 0.5 M  $\text{H}_2\text{SO}_4$  to prepare Pt or Pt-Ru solution with ratio (3)Pt:(1)Ru with the required volume and concentration. This optimized ratio gave good distribution of Pt and Ru atoms as compared to other ratios where the atoms tend to segregate forming clusters of pure Ru or Pt, thus physically separating the bi-functional metals. These solutions were used to prepare the catalyst or the mixed co-catalysts.

## 2.4. Construction of the modified electrode

For each of 8 mg ILC (optimized after several trials), 1 mL DMF was added and the solution was then ultra-sonicated until a homogeneous solution was obtained. The GC electrode was surface polished as described earlier and rinsed thoroughly with deionized water, then finally surface casted using a micropipette with 10  $\mu\text{L}$  ILC. The electrode was left for 10 min in the open air to dry the casted layer. The surface became then prepared for electrodeposition of platinum catalyst to form (GC/ILC/Pt) electrode or different co-catalysts to prepare (GC/ILC/PtRu) or (GC/ILC/PtPd) electrodes from their solutions which was performed by cyclic voltammetry (CV) in a three electrodes, one-compartment cell. Deposition of Pt and Pt-Pd was performed by applying potential between -0.25 V and +0.65V vs. 4M Ag/AgCl reference electrode at scan rate of  $50 \text{ mV s}^{-1}$  for 15 cycles. In case of Pt-Ru the CV was performed by applying potential between -1.0 V and 0.0 V vs. 4M Ag/AgCl reference

electrode at scan rate  $50 \text{ mV s}^{-1}$  for 15 cycles (Scheme 1). Furthermore, the ionic liquid modified electrode (GC/IL/PtRu) was prepared following the same procedure, by using ionic liquid (1-n-Hexyl-3-methyl imidazolium tetrafluoroborate) (IL). The electrode (GC/PtRu) was prepared by electrodeposition of PtRu co-catalysts from their solutions on GC electrode surface.



**Scheme 1.** Illustration of the synthesis steps for GC/ILC/PtRu nanocatalysts.

### 3. RESULTS AND DISCUSSION

#### 3.1. Surface characterization

The morphology of the ILC/PtRu nanocomposite was characterized by field-emission scanning electron microscopy (FE-SEM), which is shown in Figure 1A. The SEM picture shows that Pt-Ru nanoparticles are homogeneously dispersed over the surface of ILC/GCE and showed uniform formation over the ILC with the development of some clusters. In addition spherical Pt-Ru nanoparticles are showed good distribution over the surface Figure 1A (inset) due to the presence of a conductive homogenous ILC layer which helps exposing catalysis sites for methanol oxidation.

Chemical composition analysis obtained by EDX, Figure 1B confirms that Pt-Ru nanoparticles were successfully deposited on the GCE. The atomic ratio of Pt:Ru obtained by EDX analysis is approximately 3:1 which matches their original ratio in the deposition step. This indicates the uniform formation of Pt-Ru nano-composite. As a result, highly dispersed metal nanoparticles on supports with larger surface areas have advantages in catalytic activity and sensor sensitivity [28–30]. The advantage of the present method using ILC is that the size of the resulting Pt-Ru nanoparticles is relatively small and the distribution is also quite uniform and ordered.

Typical TEM image of the ILC/PtRu catalysts is shown in Figure 1C. TEM measurement showed that size distribution of Pt-Ru particles ranged in diameter between 2.0 nm and 4.0 nm, with an average diameter of around 3 nm. The formation of small size Pt-Ru nanoparticles is assisted by the underlying compact and crystalline piperidinium ionic liquid crystal layer [26, 27].

Atomic force microscope was also used to investigate the morphology of the film supported on GC. Typical 3D-images of ILC/PtRu nanocomposite are shown in Figure 1D. The surface is fairly compact with virtually no pores or cavities. The compactness and crystalline nature of the films

depicted in AFM image is due to the presence of ILC in the composite. ILC in the composite affected greatly the conductivity and gave more ordered film due to its solid state structure and its molecular orientation characteristic [31]. AFM roughness data were used to calculate the real surface area according to the following relation:

$$\text{Surface roughness} = \frac{\text{Real surface area}}{\text{Geometric surface area}} \tag{1}$$

From AFM analysis of ILC/PtRu nanocomposite, the surface roughness and real surface area were calculated and found equal to 1.08 and 0.0765 cm<sup>2</sup>, respectively.

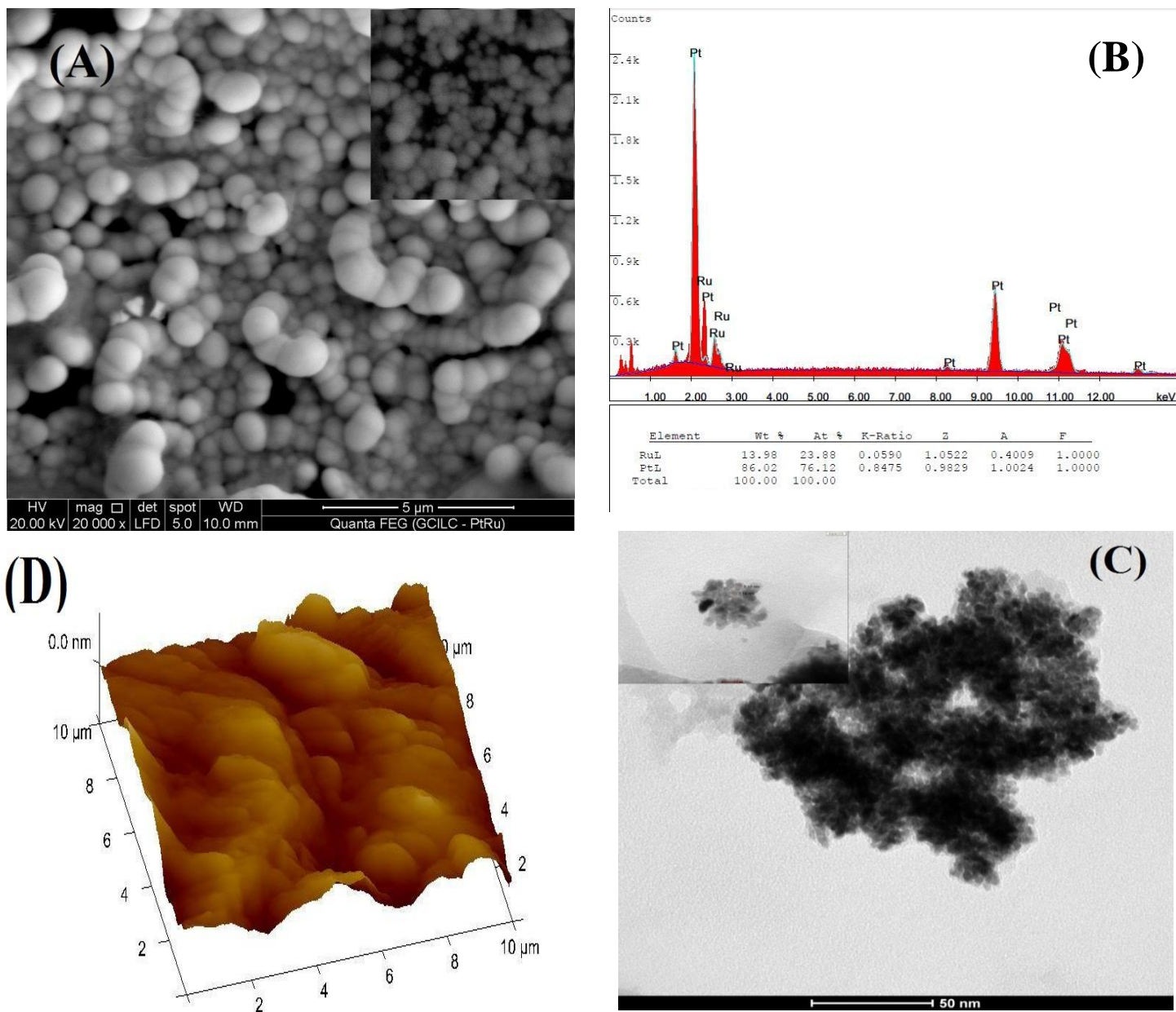


**Figure1.** (A) SEM images using FE-SEM for GC/ILC/PtRu. (B) EDAX analyses for GC/ILC/PtRu. (C) TEM images of GC/ILC/PtRu. (D) 3D-AFM images for GC/ILC/PtRu.

### 3.2. Investigation of electrocatalytic properties

The electrocatalytic oxidation of methanol at different nanocomposites modified glassy carbon namely GC/PtRu, GC/ILC/Pt, GC/ILC/PtPd and GC/ILC/PtRu was evaluated with cyclic voltammetry in a solution of 0.5 M KOH containing 0.5 M CH<sub>3</sub>OH, the scan rate is 50 mV s<sup>-1</sup>. The cyclic voltammograms were repeated until stable and reproducible CV curves were obtained in the working potential window as depicted in Figure 2.

The electro-catalytic activity of the different modified surfaces, GC/PtRu, GC/ILC/Pt, GC/ILC/PtPd and GC/ILC/PtRu towards methanol oxidation were compared. The data are reported for the forward and reverse scans with respect to oxidation peak current densities, oxidation potentials, the ratio of the forward peak current density ( $I_F$ ) to the reverse peak current density ( $I_R$ ) and the onset potential. The data are given in Table 1. The results indicated the following order of increasing of the forward oxidation potentials of methanol at the modified surfaces: GC/ILC/Pt < GC/ILC/PtRu < GC/PtRu < GC/ILC/PtPd < GC/IL/PtRu (IL is ionic liquid used for comparison with ILC). The oxidation current increased in the following order GC/ILC/Pt < GC/PtRu < GC/IL/PtRu < GC/ILC/PtPd < GC/ILC/PtRu. We concluded that the presence of ILC increases the current in presence of Pt-Ru and decreases the forward oxidation potential, while the presence of Ru lowers the potential for methanol adsorption and oxidation compared to Pd. The ILC/PtRu nano-composite plays the best ability to resist CO poisoning of the catalyst with  $I_F/I_R$  ratio of 12.2 compared to other catalysts, while for Pt-Pd the  $I_F/I_R$  ratio is 9.2. This result is more efficient and faster rate of oxidation of methanol compared to other catalysts.

In case of using the GC/ILC/PtRu modified electrode, first oxidation peak appeared in forward scan at +188 mV which is attributed to the methanol oxidation. The relative high current density of the oxidation peak (about 147 mA cm<sup>-2</sup>) indicated that methanol oxidation is effectively achieved and the high electrocatalytic efficiency of the proposed nanocomposite. Upon reversing the potential scan, another small current oxidation peak appeared at -550 mV which could be related to the oxidation of CO-containing compounds resulting from incomplete oxidation of the alcohol in the forward potential scan [32]. Thus, ILC/PtRu nanocomposite shows relatively higher conversion efficiency for methanol oxidation reaction and a better resistance to surface fouling due to intermediates generated during oxidation. The ratio of  $I_F/I_R$  can be used to characterize the catalyst poisoning tolerance to CO and the presence of PtCO<sub>ads</sub> intermediates results in the activity decay of electrocatalysts intermediates[33]. Basically, a higher  $I_F/I_R$  ratio can be applied to measure the catalyst tolerance to CO poisoning [34]. ILC/PtRu nanocomposite shows a relatively high  $I_F/I_R$  ratio of 12.2 compared to other studied catalysts nanocomposites in this work. The nanocomposite plays the best ability to resist CO poisoning of the catalyst compared to other catalysts in enhanced oxidation of methanol.

From the above discussion, we concluded that the composite electrocatalysts, ILC/PtRu, have superior activity and stability for the methanol oxidation reaction (MOR) in alkaline electrolytes. The presence of ILC is the critical key to their outstanding performances. In an alkaline environment, the rate-determining step of methanol oxidation reaction (MOR) on Pt is the oxidative removal of surface adsorbed carbonaceous intermediates, for example, CO, with the assistance of OH<sup>-</sup>. Free OH<sup>-</sup> ions in alkaline electrolytes could participate in this reaction via more predominant pathway. This is suggested

to be reactions with  $\text{OH}_{\text{ad}}^-$  species either on or around Pt sites via the Langmuir–Hinshelwood mechanism [35]. If sufficient  $\text{OH}_{\text{ad}}^-$  species are supplied nearby, the rate determining step can be greatly accelerated, and as a result, forms the basis for designing Pt alloys (including Pt-Ru), Pt-metal oxide hybrids for MOR electrocatalysis.

The resulting morphology of the ILC/PtRu nanocomposite indicated that spaces between the Pt-Ru nanoparticles were covered with ILC, the particles quite separated from each other [28], and showed more available Pt sites for methanol oxidation and those of Ru for more oxidative removal of carbonaceous poison. Furthermore, ILC in the composite affected greatly the conductivity and gave more homogenous film for electro-deposition of the nanocatalysts in ordered form due to its solid state structure and its molecular orientation ordering characteristic [36], [37]. On the other hand, it decreases the aggregation of the nanocatalysts over the surface and it allows increasing in  $\text{OH}^-$  ions availability at the vicinity of the catalysis sites.

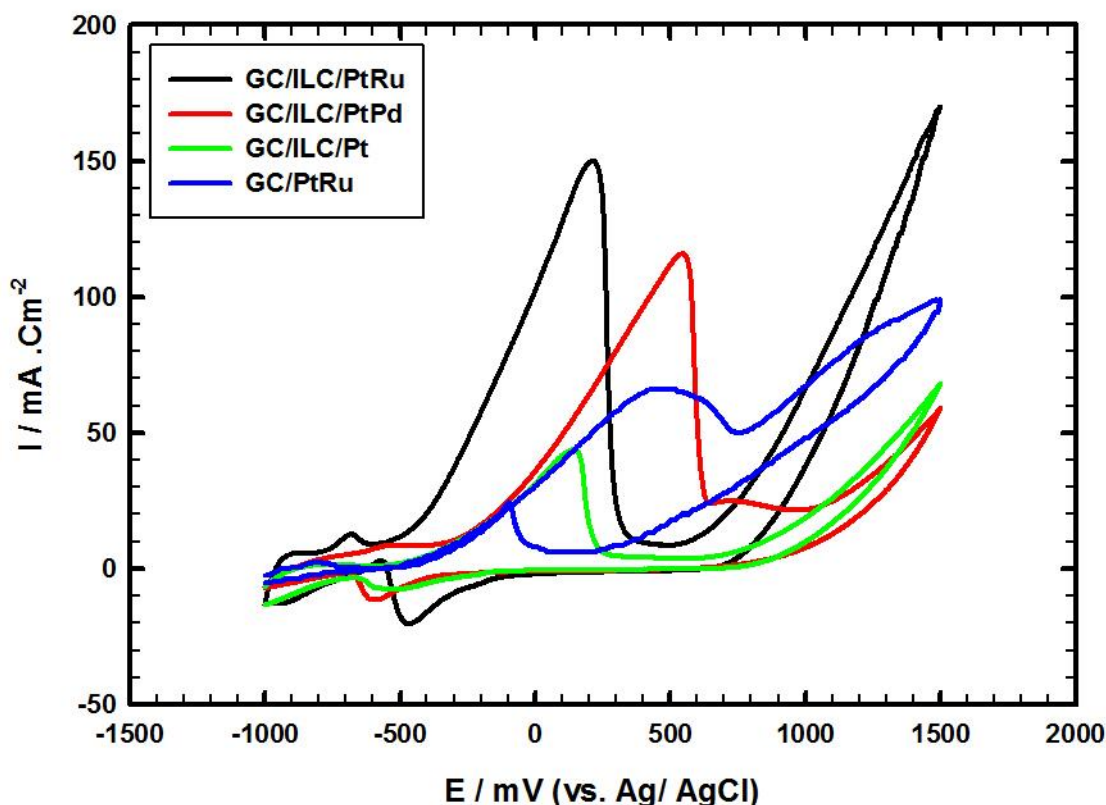


**Figure 2.** CVs of GC/ILC/PtRu, GC/ILC/PtPd, GC/ILC/Pt and GC/PtRu in the solution of 0.5 M KOH containing 0.5M  $\text{CH}_3\text{OH}$  at a scan rate of  $50 \text{ mV s}^{-1}$ .

Theoretical consideration suggests that at lower values of potential application, C-H breaks and intermediate species as CO are removed from the surface [38]. Therefore, at lower potential values C-H bonds break easier and oxidation products are less likely to adsorb to the surface. It was reported earlier reached [39], that the onset being defined as the potential at which 10% or 20% of the current density value at the peak potential was reached. As can be noticed from Figure 2, the onset potential of methanol oxidation over GC/ILC/PtRu was  $-570 \text{ mV}$ , which is more negative compared to other

studied nanocatalysts composites. This reveals that GC/ILC/PtRu nanocomposite exhibited better performance for the promotion of C–H breaking compared to the other modified nanocatalysts composites. The synergy between Pt-Ru and ILC is also shown to promote CO oxidation, leading to a significant reduction of the reaction onset overpotentials [40]. In light of the diverse effects on MOR, we propose that the bi-functional interaction between Pt and Ru in presence of ILC may present a possible solution to the long- standing durability issue in methanol oxidation.

To further evaluate the performance of the proposed novel nanocomposite (GC/ILC/PtRu), some relevant reported literature is listed in Table 2 for comparison. The proposed naocomposite ILC/PtRu displayed higher catalytic performance for methanol oxidation and intermediates tolerance in comparison to other composites reported in the literature. On the basis of these results, we can conclude that the ILC played an important role in facilitating the methanol oxidation reaction and tolerance to intermediates such as CO poisoning for Pt based catalyts.

**Table1.** Comparison of electrocatalytic activity of methanol oxidation on GC/PtRu, GC/IL/PtRu, GC/ILC/Pt, and GC/ILC/PtPd and GC /ILC /PtRu nanocatalysts

Electrode	Forward potential (mV)	Forward Current (mA/cm <sup>2</sup> )	Onset potential (mV)	IF/IR
GC/PtRu	435	72.1	-400	3.1
GC/IL/PtRu	605	91.2	-500	3.0
GC/ILC/Pt	116	46.3	-480	5.7
GC/ILC/PtPd	512	125.2	-300	9.2
GC/ILC/PtRu	188	146.9	-570	12.3

### 3.3. Comparison between ionic liquid and ionic liquid crystal modified electrodes

The performance of the GC/ILC/PtRu electrode was compared to GC/IL/PtRu electrode toward MOR. Thus, CVs were performed in the solution of 0.5 M KOH containing 0.5 M CH<sub>3</sub>OH at scan rate 50 mV s<sup>-1</sup>. As can be noticed from Figure 3, the onset potential of methanol oxidation using GC/ILC/PtRu nanocatalysts was -570 mV, which is more negative than GC/IL/PtRu nanocatalysts (-500 mV). The peak current density observed at GC/ILC/PtRu nanocatalysts is approximately 146.9 mA cm<sup>-2</sup>, which is noticeably higher than that at GC/IL/PtRu nanocatalysts (ca. 91.2 mA cm<sup>-2</sup>). Also GC/ILC/PtRu nanocatalysts has an I<sub>F</sub>/I<sub>R</sub> ratio of 12.2, which is again much higher than that of GC/IL/PtRu nanocatalysts (ca. 3.0). These results suggest that ILC displays the best ability to resist CO poisoning, facilitating the methanol oxidation process and performance for the promotion of C–H breaking compared to IL-modified electrodes. Moreover, the utilization of ILC tends to lower the forward oxidation potential peak significantly (ca. 188 mV) than that at GC/IL/PtRu (ca. 605 mV). So we can conclude that the ILC plays an important role due to higher enhancement and faster charge transfer rate. This observation is attributed to the ionic conductivity and the solid state structure of the ionic liquid crystal which helps in the formation of ordered films[41], [42]. Furthermore, certain ionic materials are known also to form amphiphilic liquid crystals. In such case, a wider electrochemical potential window is obtained as the positive charge is localized on the nitrogen atom of piperidinium

salts than in case of imidazolium and pyridinium salts at which the positive charge is delocalized over the aromatic ring.

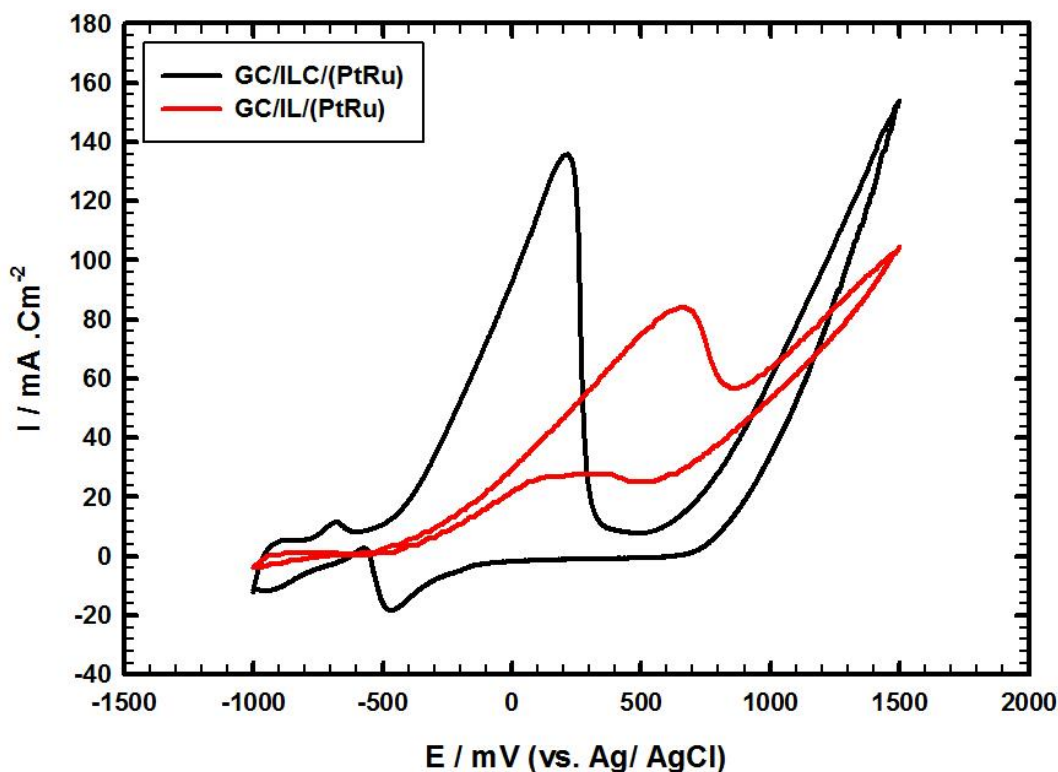


**Figure 3.** Cyclic voltammograms of GC/ILC/PtRu and GC/IL/PtRu in the solution of 0.5 M KOH containing 0.5M CH<sub>3</sub>OH at a scan rate of 50 mV s<sup>-1</sup>.

### 3.4. Investigation of stabilities of the modified surfaces

From the practical point of view, stability is one of the critical factors for DMFCs catalyst. The electrochemical stability and durability of GC/ILC/PtRu and GC/PtRu catalysts were characterized by amperometric (I-t relation) experiments in 0.5 M KOH containing 0.5 M CH<sub>3</sub>OH Figure 4A. During the methanol oxidation processes, some intermediate species such as CO and CHO are generated on the catalysts surface, which could significantly poison the catalyst and thus hinder the methanol oxidation [43]. All catalysts showed a fast current decrease in the first steps of the process; thereafter all catalysts exhibited a steady-state current response with time. The current density generated from GC/ILC/PtRu nanocatalysts was higher compared to GC/PtRu nanocatalysts during the whole testing process. As can be observed, excellent stability for GC/ILC/PtRu was obtained for over 1 hour while in case of GC/PtRu deviation started gradually after 30 min. Further investigation is performed via repeated cycle stability of the GC/ILC/PtRu nanocatalysts towards methanol oxidation reaction; CVs of 25 cycles have been performed in the solution of 0.5 M KOH containing 0.5 M CH<sub>3</sub>OH at 50 mV s<sup>-1</sup> Figure 4B. The results illustrate that ILC as support can improve the electrocatalytic activity and further the stability of the composite.

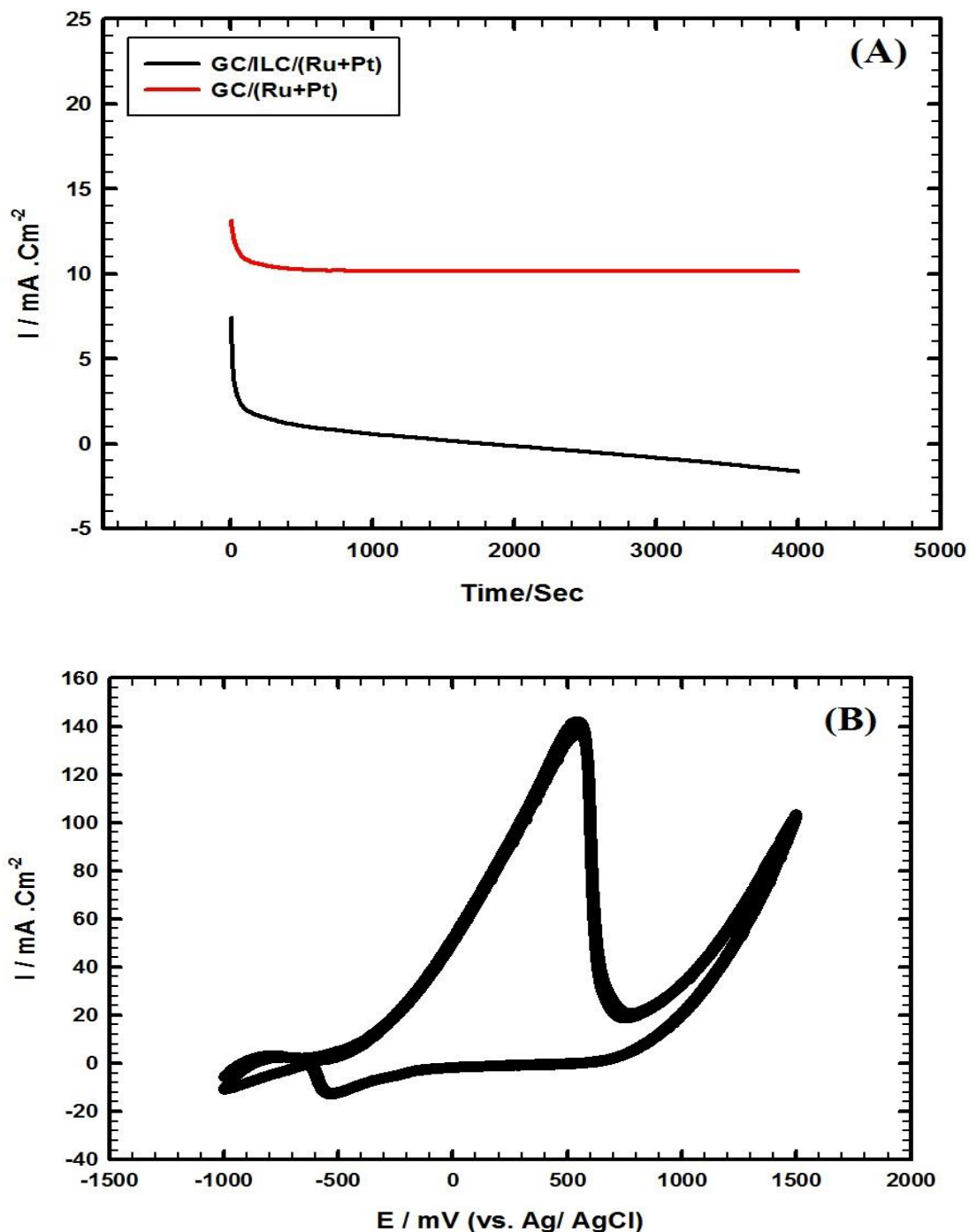


**Figure 4.** (A) Amperometric *i-t* Curve of GC/ILC/PtRu and GC/PtRu nanocatalysts was held at -0.15 V for 4000 s in the solution of 0.5 M KOH containing 0.5 M CH<sub>3</sub>OH. (B) CVs of repeated cycles in the solution of 0.5 M KOH containing 0.5M CH<sub>3</sub>OH at a scan rate of 50 mV s<sup>-1</sup> recorded at GC/ILC/PtRu.

### 3.5. Effect of co-catalyst loading

The amount of loaded Pt-Ru nanoparticles could be easily controlled via simply changing the number of scanning cycles (by changing the amount of charge used for electrodeposition), thus

resulting in the tunable catalytic properties [44]. In Figure 5 the results showed that as the number of repeated cycles during Pt-Ru deposition increases, the anodic peak current of methanol oxidation increases. This was realized up to 15 cycles after which the methanol oxidation peak current densities became nearly stable. On the basis of these results, 15 scanning cycles were selected for preparing Pt-Ru nanocatalysts which has lower oxidation potential and maximum current. From an economical point view, this was also desirable for commercial use.

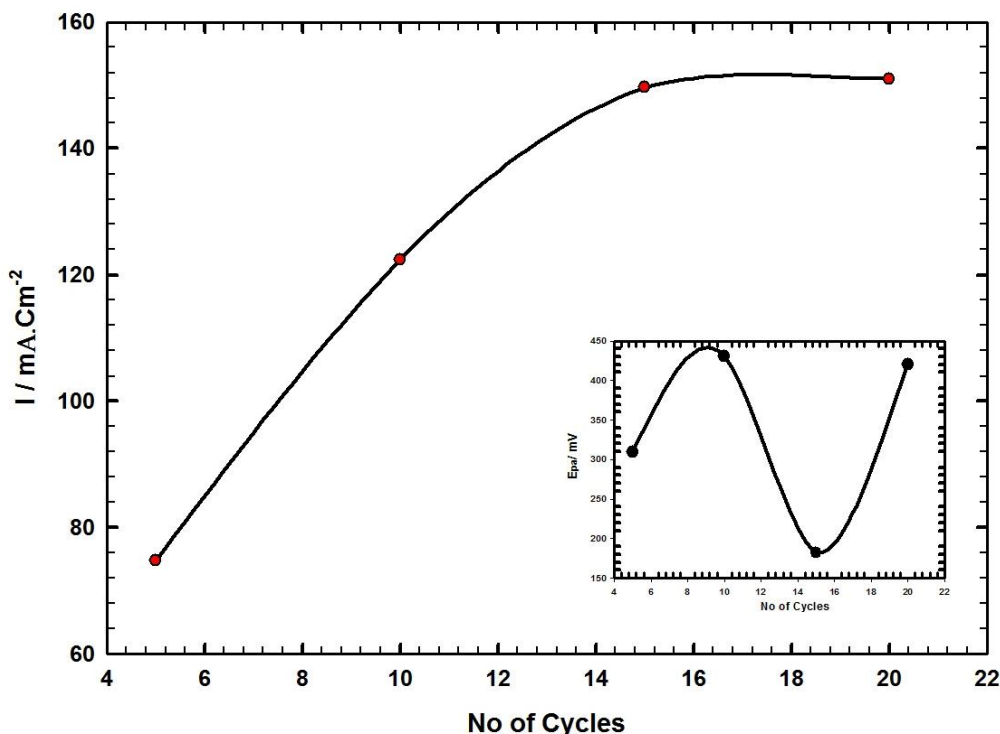


**Figure 5.** Effect of co-catalyst loading on peak current density of methanol oxidation with different scanning cycles for electrodepositing Pt-Ru at GC/ILC/PtRu in the solution of 0.5 M KOH containing 0.5M CH<sub>3</sub>OH at a scan rate of 50 mV s<sup>-1</sup>. Inset: Variation of the peak potential of methanol oxidation at different scanning cycles

### 3.6. Effect of scan rate on the electrochemical behavior of GC/ILC/PtRu

Cyclic voltammograms of GC/ILC/PtRu in the solution of 0.5 M KOH containing 0.5 M CH<sub>3</sub>OH at different scan rates from 10 to 1000 mVs<sup>-1</sup> are shown in Figure 6 (inset A). With an increase in the scan rate, the peak current ( $I_p$ ) increased and the anodic peak potential shifted to more positive value. Figure 6 illustrates the plot of anodic peak current ( $I_{\text{pa}}$ ) against the square root of the scan rate ( $v^{1/2}$ ). It can be seen that the anodic peak current are linearly proportional to  $v^{1/2}$ , indicating that the electrode reaction is limited by diffusion. The oxidation peak potential ( $E_p$ ) rises linearly with  $\log(v)$  indicating that the oxidation of methanol is an irreversible reaction process Figure 6 (inset B) [14]. In general, the relationship between  $E_p$  and  $\log(v)$  can be represented with the following equation [45][46]:

$$K = \frac{\partial E_p}{\partial \log(v)} = \frac{2.3RT}{(1-\alpha)nF} \tag{2}$$

Where,  $\alpha$  is the electron transfer coefficient, characterizing the effect of electrochemical potential on the activation energy of an electrochemical reaction [45],[46]. Hence,  $\alpha$  value was calculated as 0.52 for GC/ILC/PtRu nanocatalysts .This demonstrated that GC/ILC/PtRu nanocatalysts have small activation energy and thus enhanced kinetics for methanol oxidation. Diffusion coefficients of methanol at GC/ILC/PtRu and GC/PtRu are  $2.96 \times 10^{-6} \text{ cm}^2 \text{ s}^{-1}$  and  $0.0133 \times 10^{-6} \text{ cm}^2 \text{ s}^{-1}$ , respectively. This indicates faster diffusion process of methanol at the surface of GC/ILC/PtRu.

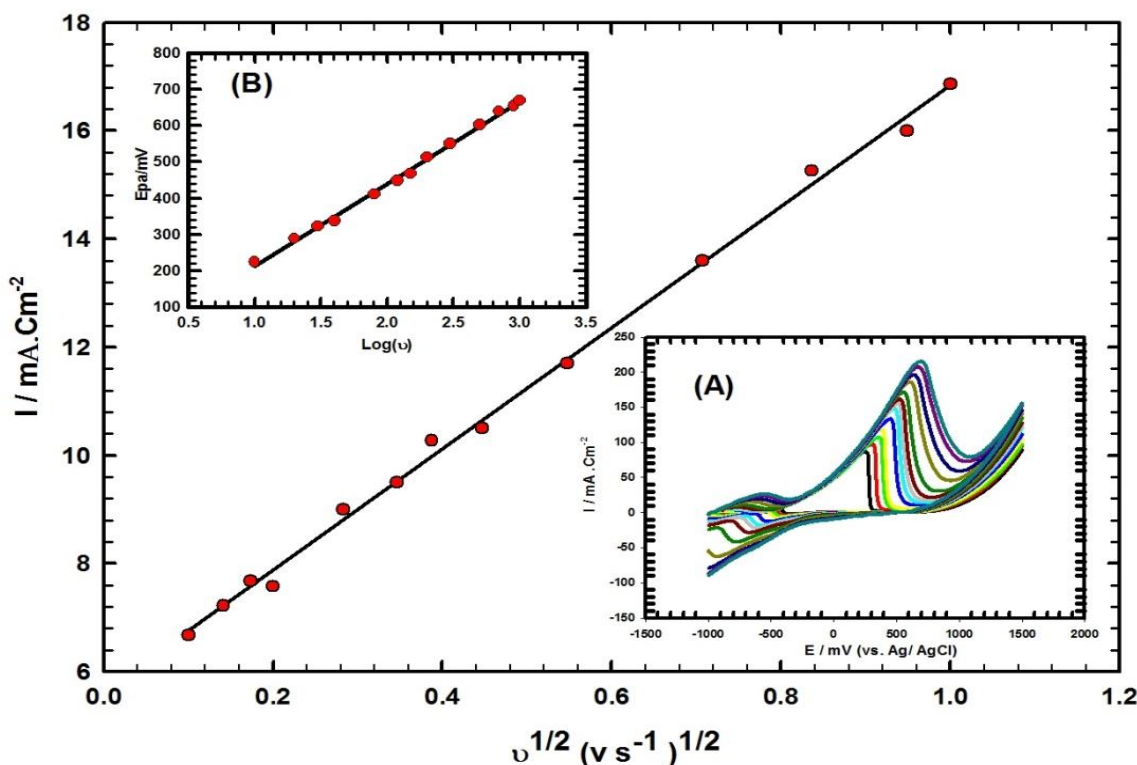


**Figure 6.** The relationship between the peak current density value of the methanol oxidation and the square root of scan rate ( $v^{1/2}$ ) of GC/ILC/PtRu nanocatalysts in the solution of 0.5 M KOH containing 0.5 M  $\text{CH}_3\text{OH}$ . Inset (A) CVs of GC/ILC/PtRu nanocatalysts at the different scan rates from 10 to 1000  $\text{mVs}^{-1}$ . Inset (B) The relationship between the peak potential  $E_{pa}$  of the methanol oxidation and  $\log(v)$ .

### 3.7. Effect of methanol concentration

Evaluation of the presence of ILC in the modified composite at high methanol concentrations was studied. The dependence of peak current densities on the concentration of methanol ranging from 0.05 M to 1.5 M using both electrodes GC/ILC/PtRu and GC/PtRu are shown in Figure 7. The results show that the current response for GC/PtRu reaches steady state after 0.4 M methanol, while in case of GC/ILC/PtRu linear relationship is obtained by plotting anodic peak current versus concentration of the methanol. This linear relation confirmed that GC/ILC/PtRu resists the accumulation of

electrooxidation products at high methanol concentrations and consequently can be applied for different “fuel” concentrations.

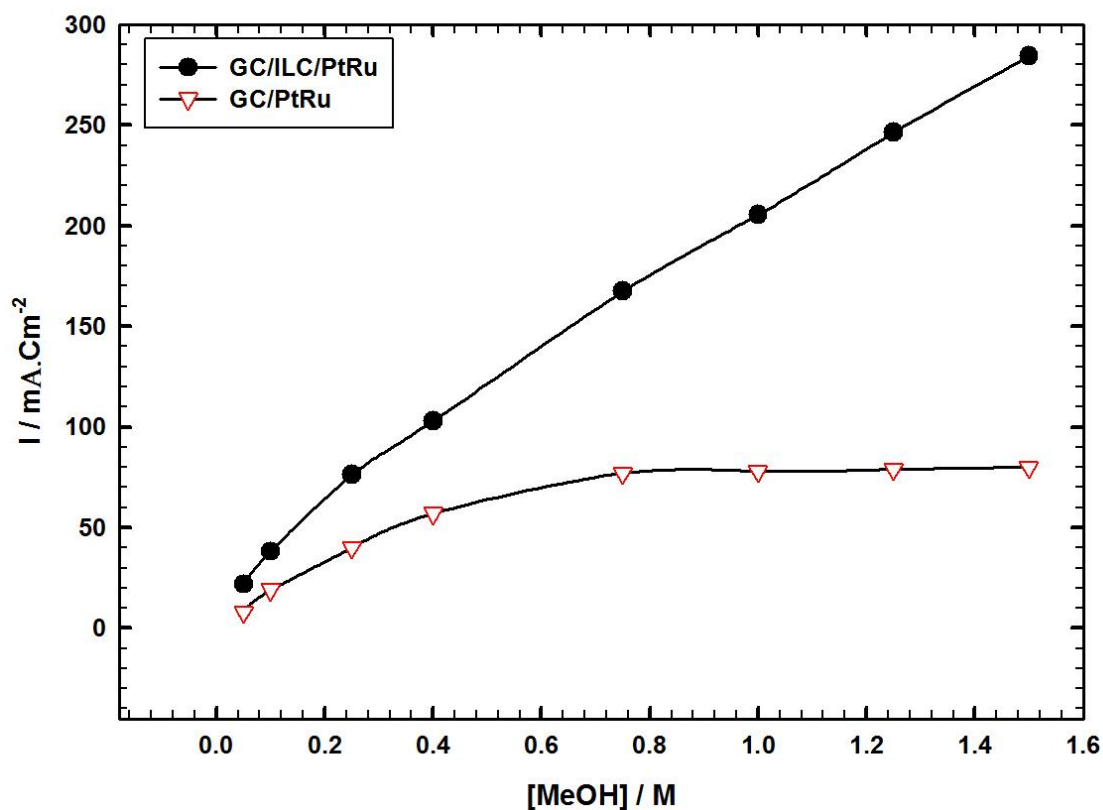


**Figure 7.** The peak current density value of the methanol oxidation at the GC/ILC/PtRu and GC/PtRu electrodes in 0.5 M KOH solution containing different concentrations of methanol at a scan rate of  $50 \text{ mV s}^{-1}$ .

### 3.8. Effect of temperature

Effect of temperature changes on both GC/ILC/PtRu and GC/PtRu performance in 0.5 M  $\text{CH}_3\text{OH} + 0.5 \text{ M KOH}$  was studied. Figure 8 shows the Arrhenius plot of methanol oxidation in the temperature range from 5 to  $60 \text{ }^\circ\text{C}$ . The peak current value increases as the temperature increased up to  $60 \text{ }^\circ\text{C}$  which indicates that the mechanism of methanol oxidation at the surface of GC/ILC/PtRu and GC/PtRu is partially activation controlled. The decrease of peak current value at higher temperatures can be attributed to the progressive evaporation of methanol (the boiling point of methanol is  $64.5^\circ\text{C}$ ) with increasing temperature. By assuming that no azeotrope is formed in the methanol/water mixture [47], it is expected that a progressive decrease in peak current should appear during the temperature elevation, because of a loss in methanol concentration. By plotting  $\log I_{pa}$  (anodic peak current) versus reciprocal of temperature we can calculate the value of activation energy,  $E_a$ , as indicated in Figure 8. The calculated  $E_a$  using GC/ILC/PtRu is  $12.89 \text{ kJ mol}^{-1}$  while the  $E_a$  value using GC/PtRu is  $23.26 \text{ kJ mol}^{-1}$ . The smaller activation energy in case of GC/ILC/PtRu electrode is due to the special synergism between the components of the nanocomposite and ILC resulting in higher electrocatalytic behavior of GC/ILC/PtRu compared to GC/PtRu toward methanol oxidation.

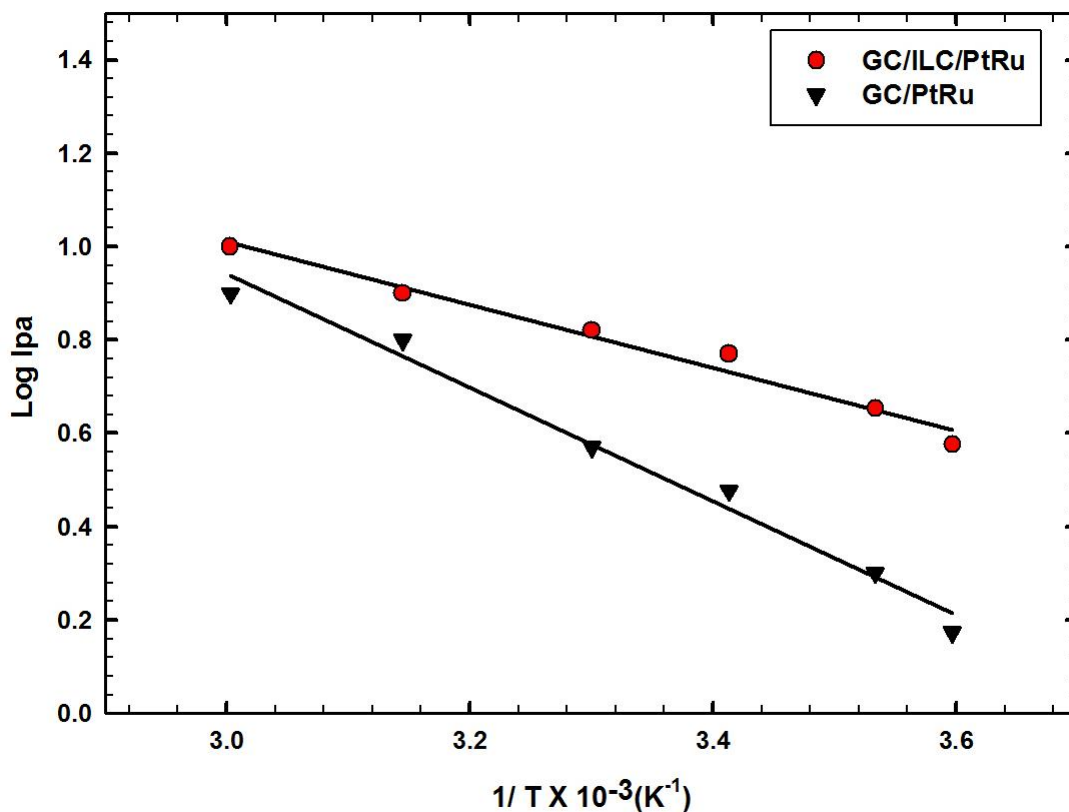


**Figure 8.** Arrhenius plot of log (Ipa) versus  $T^{-1}$  at GC/ILC/PtRu and GC/PtRu electrodes in 0.5 M KOH solution containing 0.25 M CH<sub>3</sub>OH at a scan rate of 50 mVs<sup>-1</sup>.

**Table 2.** Comparison of the peak potential and the peak current density reported for methanol electro-oxidation on various electrodes

Electrode	Forward potential (mV)	Forward Current (mA/cm <sup>2</sup> )	Methanol Concentration (M)	Medium	Reference
GC/Ni(II)OPD	570 vs. SCE	10.2	0.10	Basic	[48]
GC /Ni(II)-DHS	626 vs. SCE	3.1	0.10	Basic	[49]
GC/PolyNi(II)TCPP	680 vs. SCE	2.23	0.10	Basic	[50]
GC/Ni(II)CosalenA	580 vs. SCE	7.05	0.35	Basic	[51]
GC /Ni-Co	600 vs. Ag/AgCl	2.3	0.10	Basic	[52]
GC /Ni-Cu	600 vs. Ag/AgCl	35	0.30	Basic	[53]
GC /Ni-ZnsalenA	569 vs. SCE	6.7	0.35	Basic	[54]
GC/ILC/PtRu	188 vs. Ag/AgCl	146.9	0.50	Basic	Our work

NiOPD: Bis(1,2-phenylenediamine)Nickel(II), DHS: N,N'-bis(2,5-dihydroxybenzylidene)-1,2-diaminobenzene, TCPP: tetra(4-carboxyphenyl)porphyrin, Salen: (N,N-bis(salicylidene)ethylenediamine)

#### 4. CONCLUSIONS

In our conclusion, we report a novel ILC/PtRu nanocomposite featured with PtRu nanostructures electrodeposited and supported on conductive ILC layer. The formation of Pt-Ru nanoparticles is due to compactness and crystalline nature of piperidinium ionic liquid crystal. Furthermore, the incorporation of ILC greatly facilitates the presence of available Pt and Ru active sites by keeping them quite separated from each other. This morphology enhances the methanol oxidation process and subsequently assists in the oxidative removal of carbonaceous poison via the Langmuir–Hinshelwood reaction pathway. The synergism between the main three components of the composite materials achieves impressive methanol oxidation reaction activity and long-term durability far better than those previously reported in the literature. The ILC/PtRu nanocomposite for electrocatalysis of methanol oxidation reaction represents a promising highly efficient performance for their commercial applications in DMFCs.

#### ACKNOWLEDGEMENT

The authors express their gratitude to the University of Cairo (Office of Vice President for Graduate Studies and Research) for providing partial financial support.

#### References

1. T. Iwasita, *Electrochim. Acta*, 47 (2002) 3663.
2. H. Nonaka, Y. Matsumura, *J. Electroanal. Chem.*, 520 (2002) 101.
3. M. Fleischmann, K. Korinek, D. Pletcher, *J. Electroanal. Chem. Interfacial Electrochem.*, 31 (1971) 39.
4. H. Heli, M. Jafarian, M.G. Mahjani, F. Gobal, *Electrochim. Acta*, 49 (2004) 4999.
5. T.J. Schmidt, H.A. Gasteiger, R.J. Behm, *Electrochem. Commun.*, 1 (1999) 1.
6. E. Antolini, *Energy Environ. Sci.*, 2 (2009) 915.
7. A. Chen, P. Holt-Hindle, *Chem. Rev.*, 110 (2010) 3767.
8. Y. Morimoto, E.B. Yeager, *J. Electroanal. Chem.*, 444 (1998) 95.
9. S. Du, Y. Lu, R. Steinberger-Wilckens, *Carbon N. Y.*, 79 (2014) 346.
10. G. Shi, Z. Wang, J. Xia, J. Tang, F. Zhang, Y. Li, Y. Xia, L. Xia, *Int. J. Electrochem. Sci.*, 8 (2013) 8764.
11. H.A. Gasteiger, N. Markovic, P.N. Ross Jr, E.J. Cairns, *J. Phys. Chem.*, 97 (1993) 12020.
12. O.A. Petrii, *Dokl. Akad. Nauk SSSR*, 160 (1965) 871.
13. V.S. Entina, O.A. Petri, *Elektrokhimiya*, 4 (1968) 678.
14. Z. Wang, G. Shi, J. Xia, Y. Xia, F. Zhang, L. Xia, D. Song, J. Liu, Y. Li, L. Xia, others, *Electrochim. Acta*, 121 (2014) 245.
15. H. Ji, M. Li, Y. Wang, F. Gao, *Electrochem. Commun.*, 24 (2012) 17
16. H.K. Hassan, N.F. Atta, A. Galal, *J. Solid State Electrochem.*, 17 (2013) 1717.
17. U. Kernchen, B. Etzold, W. Korth, A. Jess, *Chem. Eng. Technol.*, 30 (2007) 985.
18. J. Arras, E. Paki, C. Roth, J. Radnik, M. Lucas, P. Claus, *J. Phys. Chem. C.*, 114 (2010) 10520.
19. J. Arras, M. Steffan, Y. Shayeghi, P. Claus, *Chem. Commun.*, (2008) 4058.
20. F. Schwab, N. Weidler, M. Lucas, P. Claus, *Chem. Commun.*, 50 (2014) 10406.
21. C. Meyer, V. Hager, W. Schwieger, P. Wasserscheid, *J. Catal.*, 292 (2012) 157.
22. T. Mangartz, L. Haecker, W. Korth, C. Kern, A. Jess, *OIL GAS-EUROPEAN Mag.*, 40 (2014) 84.
23. J. Snyder, T. Fujita, M.W. Chen, J. Erlebacher, *Nat. Mater.*, 9 (2010) 904.

24. J. Snyder, K. Livi, J. Erlebacher, *Adv. Funct. Mater.*, 23 (2013) 5494.
25. G.-R. Zhang, M. Munoz, B.J.M. Etzold, *ACS Appl. Mater. Interfaces*, 7 (2015) 3562.
26. Q. Zhang, L. Jiao, C. Shan, P. Hou, B. Chen, X. Xu, L. Niu, *Liq. Cryst.*, 35 (2008) 765.
27. Q. Zhang, C. Shan, X. Wang, L. Chen, L. Niu, B. Chen, *Liq. Cryst.*, 35 (2008) 1299.
28. S. Kumar, S.K. Pal, *Tetrahedron Lett.*, 46 (2005) 2607.
29. N.F. Atta, H. Ekram, Y.M. Ahmed, A. Galal, *Electrochim. Acta*, 199 (2016) 319.
30. N.F. Atta, A.H. Ibrahim, A. Galal, *New J. Chem.*, 40 (2016) 662.
31. H. Zhang, H. Cui, *Langmuir*, 25 (2009) 2604.
32. M.S. Wietecha, J. Zhu, G. Gao, N. Wang, H. Feng, M.L. Gorrington, M.L. Kasner, S. Hou, *J. Power Sources*, 198 (2012) 30.
33. C.H. Yen, K. Shimizu, Y.-Y. Lin, F. Bailey, I.F. Cheng, C.M. Wai, *Energy & Fuels*, 21 (2007) 2268.
34. Y. Xing, *J. Phys. Chem. B.*, 108 (2004) 19255.
35. T. Frelink, W. Visscher, J. a R. Van Veen, *Surf. Sci.*, 335 (1995) 353.
36. N.F. Atta, H. Ekram, A. Galal, *J. Electrochem. Soc.*, 163 (2016) B325.
37. N.F. Atta, S.S. Elkholy, Y.M. Ahmed, A. Galal, *J. Electrochem. Soc.*, 163 (2016) B403.
38. X. Chen, Z. Cai, X. Chen, M. Oyama, *Carbon*, 66 (2014) 387.
39. F. Maillard, A. Bonnefont, M. Chatenet, L. Guétaz, B. Doisneau-Cottignies, H. Roussel, U. Stimming, *Electrochim. Acta*, 53 (2007) 811.
40. R. Subbaraman, D. Tripkovic, K.-C. Chang, D. Strmcnik, A.P. Paulikas, P. Hirunsit, M. Chan, J. Greeley, V. Stamenkovic, N.M. Markovic, *Nat. Mater.*, 11 (2012) 550.
41. M. Shukla, S. Saha, A Comparative Study of Piperidinium and Imidazolium Based Ionic Liquids: Thermal, Spectroscopic and Theoretical Studies, *INTECH Open Access Publisher*, 2013.
42. K. Lava, (2012).
43. Z. Cai, C. Liu, G. Wu, X. Chen, X. Chen, *Electrochim. Acta*, 127 (2014) 377.
44. R. Ojani, J.-B. Raoof, M. Goli, R. Valiollahi, *J. Power Sources*, 264 (2014) 76.
45. W. Ye, H. Kou, Q. Liu, J. Yan, F. Zhou, C. Wang, *Int. J. Hydrogen Energy*, 37 (2012) 4088.
46. H. Tang, J. Chen, S. Yao, L. Nie, Y. Kuang, Z. Huang, D. Wang, Z. Ren, *Mater. Chem. Phys.*, 92 (2005) 548.
47. S. Ohi, (1989).
48. A.N. Golikand, S M Golabi, M. Ghannadi Maragheh, L. Irannejad, M. Asgari, *Chem. Soc.*, 4 (2007) 304.
49. M. Revenga-Parra, T. García, E. Lorenzo, F. Pariente, *Sensors Actuators B Chem.*, 130 (2008) 730.
50. M. Jafarian, M. a. A. Haghighatbin, F. Gobal, M.G.G. Mahjani, S. Rayati, *J. Electroanal. Chem.*, 663 (2011) 14.
51. W. Wang, R. Li, X. Hua, R. Zhang, *Electrochim. Acta*, 163 (2015) 48.
52. M. Asgari, M.G. Maragheh, R. Davarkhah, E. Lohrasbi, A.N. Golikand, *Electrochim. Acta*, 59 (2012) 284.
53. I. Danaee, M. Jafarian, F. Forouzandeh, F. Gobal, M.G. Mahjani, *Int. J. Hydrogen Energy*, 33 (2008) 4367.
54. W. Wang, R. Li, L. Liu, R. Zhang, B. Wang, *J. Solid State Electrochem.*, 19 (2015) 2001.